Beyond RSS: A PRR and SNR Aided Localization System for Transceiver-free Target in Sparse Wireless Networks

Dian Zhang, *Member, IEEE*, Wen Xie, Zexiong Liao, Wenzhan Zhu, Landu Jiang*, Yongpan Zou*

Abstract—Nowadays transceiver-free (also referred to as device-free) localization using Received Signal Strength (RSS) is a hot topic for researchers due to its widespread applicability. However, RSS is easily affected by the indoor environment, resulting in a dense deployment of reference nodes. Some hybrid systems have already been proposed to help RSS localization, but most of them require additional hardware support. In order to solve this problem, in this paper, we propose two algorithms, which leverage the Packet Received Rate (PRR) to help RSS localization without additional hardware support. Moreover, we take the environment noise information into consideration by utilizing the Signal-to-Noise Ratio (SNR) which is based on the RSS and Noise Floor (NF) information instead of pure RSS. Thus, we can alleviate the noise effect in the environment and make our system more sensitive to the target. Specifically, when reference nodes are sparsely deployed and RSS is very weak, PRR and SNR can help in performing localization more accurately. Our BEYOND RSS system is based on sparse wireless sensor networks, wherein the experimental results show that the average localization error of our approach outperforms the pure RSS based approach by about 15.19%.

Index Terms—Transceiver-free localization, PRR, RSS, SNR, NF, None-Line-of-Sight.

✦

1 INTRODUCTION

INDOOR localization can help users navigate indoors in closed spaces that are not covered by Global Positioning System (GPS). Existing localization can be divided into two categories: Transceiver-based (also referred to as device-based) and transceiver-free (also referred to as device-free). Device-based technologies require the target to carry a wearable device (e.g. an RFID tag) [1], [2]. Such requirement may not be satisfied in certain real-world applications, e.g., the security monitoring system.

Transceiver-free localization is able to localize target without carrying any device. Among the technologies to localize the transceiver-free target, Radio Frequency (RF) based technologies remain a hot topic in the research field since they can be applied in various scenarios without many limitations on the environments and users, e.g., the light requirement and privacy concern.

Traditional RF-based technologies usually leverage the

Dian Zhang is an associate professor in the Department of Computing & Decision Sciences, Lingnan University, 8 Castle Peak Road, Tuen Mun, New Territories, Hong Kong, e-mail: serena.dian@gmail.com
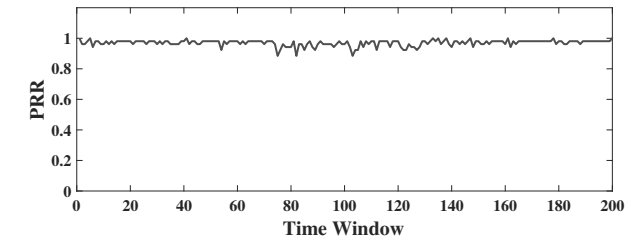
Wen Xie is a postgraduate student in the Department of Computer Science and Software Engineering, Shenzhen University, 3688 Nanhai Avenue, Shenzhen, P.R. China, e-mail: 1810273027@email.szu.edu.cn

Zexiong Liao is a postgraduate student in the Department of Computer Science and Software Engineering, Shenzhen University, 3688 Nanhai Avenue, Shenzhen, P.R. China, e-mail: 1810273017@email.szu.edu.cn
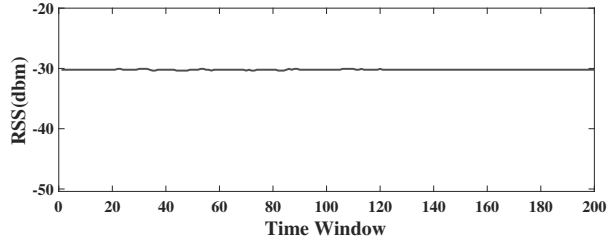
Wenzhan Zhu is a research assistant in the Department of Computer Science and Software Engineering, Shenzhen University, 3688 Nanhai Avenue, Shenzhen, P.R. China, e-mail: 2829577527@qq.com

Landu Jiang is an associate researcher in the Department of Computer Science and Software Engineering, Shenzhen University, 3688 Nanhai Avenue, Shenzhen, P.R. China, e-mail: landu.jiang@mail.mcgill.ca. He is a corresponding author
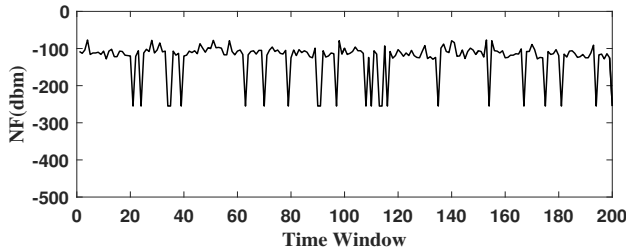
Yongpan Zou is an assistant professor in the Department of Computer Science and Software Engineering, Shenzhen University, 3688 Nanhai Avenue, Shenzhen, P.R. China, e-mail: yongpan@szu.edu.cn. He is a corresponding author

signal variance, which is affected by the target in localization. Radio Signal Strength (RSS) and Channel State Information (CSI) are the two types of mostly adopted resources. Some WiFi-based positioning systems [3]–[12] using CSI can locate the transceiver-free target with only two signal transceivers. However, CSI is the physical layer information, which is not available in most common devices.

RSS is widely used because it is regarded as a free source and can be obtained from almost all the common devices. However, the greatest disadvantage of RSS-based localization is that the RSS signal is easy to be influenced by a slight variation in the environment and its effect depends on the link quality. If the environment has much noise [13], this situation becomes worse. Therefore, many RSS-based localization methods require the dense deployment of the reference nodes [14] [15] [16]. But if in a complicate indoor area, even the distance between the two nodes is not very far, the link quality can become unstable due to the interference of indoor objects. There are also some fingerprinting technologies based on sparse deployment [17] [18]. By and large, the traditional transceiver-free indoor localization methods require at least 3 communication nodes in a limited experimental area [14]. However, the link quality is more susceptible to interference and becomes unstable, causing reduced the localization accuracy. Traditional fingerprinting algorithms can also work in the sparse deployment [19] [20] [21] [22]. However, the link quality plays a critical role in localization. Since the link quality is more susceptible to interference, the localization accuracy is reduced and the deployed environment usually can not be very sparse. Our previous approach [18] is able to localize target in sparse deployment. But it only utilized K-Nearest Neighbor (KNN) based on Packet Received Rate (PRR), the impact of noise is not fully considered and the algorithms can be
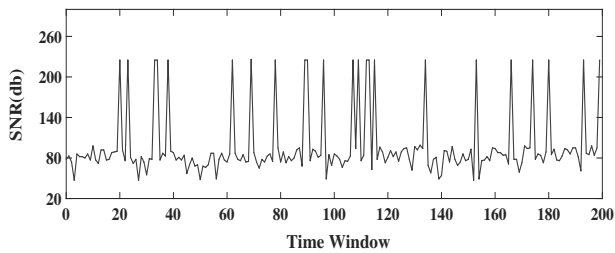
(a) PRR when no transceiver-free target appears.

(b) RSS when no transceiver-free target appears.
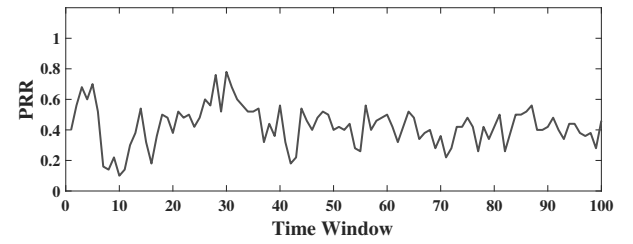
(c) NF when no transceiver-free target appears.

(d) SNR when no transceiver-free target appears.

Fig. 1: PRR vs. RSS vs. NF vs. SNR when no transceiver-free target appears.

(a) PRR when transceiver-free target appears.

(b) RSS when transceiver-free target appears.
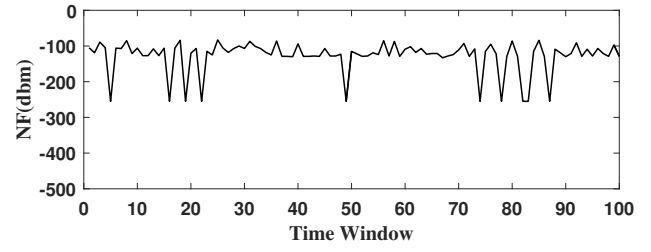
(c) NF when transceiver-free target appears.
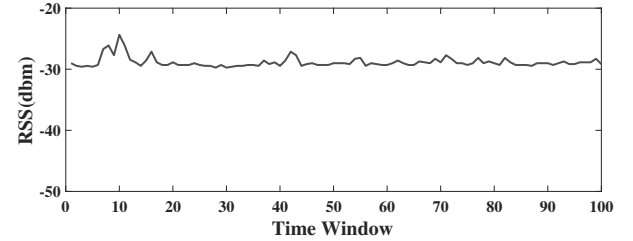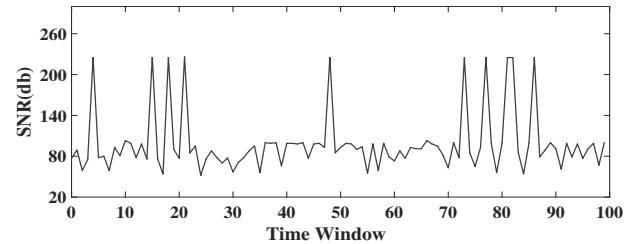
(d) SNR when transceiver-free target appears.

Fig. 2: PRR vs. RSS vs. NF vs. SNR when transceiver-free target appears.

improved. There are also some hybrid systems utilizing other resources, e.g. ultrasound, image, infrared sensors, in localization [23] [24] [25] [26] [27] [28]. These systems not only reduce the number of RF transceivers but also provide more information compared to pure RF-based systems. But all these above systems usually require additional hardware support. The work by X. Huang et al. [29] used PRR to recognize human motion. It has not been successfully applied in localization, but it has not been successfully applied in localization.

In order to solve the above problem, in this paper, we propose a fine-grained localization system BEYOND RSS, which is able to accurately localize transceiver-free targets in sparse networks without introducing additional hardware support. Even in an environment where the signal is very weak and more susceptible to interference, our approach

can alleviate the noise effect and are more sensitive to the target, so that the performance can still is improved.

Our basic idea is based on the following observations as shown in Figure 1. We find that, when RSS is weak, no matter whether the target object is in the environment or not, the PRR is more sensitive than RSS and shows larger fluctuation range. Such PRR fluctuation often occurs in the transition region [30] [31] when the link quality is unstable. Therefore, our basic idea is to introduce Packet Received Rate (PRR) as an additional resource, and use Signal-to-Noise Ratio (SNR) [32] [33] instead of traditional pure RSS to localize target nodes, as PRR and SNR can play a constructive role in the localization and be the mutually successful partnership in this situation.

In our BEYOND RSS system, we propose two localization algorithms. The first one is based on Dynamic Time
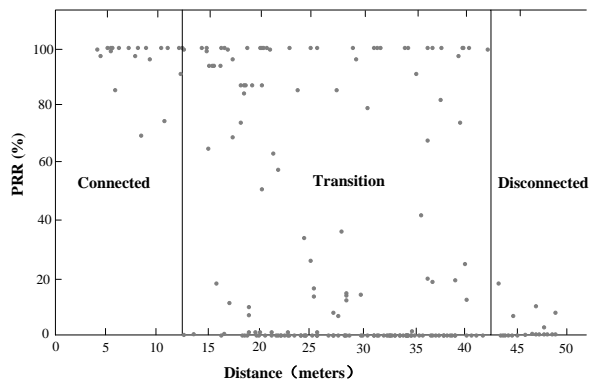
Fig. 3: Transition region: when the distance between nodes is not large, usually the PRR is stabilized at 100% (link quality is stable). But when the distance grows larger, the RSS becomes very weak while the link still connects (unstable link quality). In such a situation, the PRR value may vary, which is known as transitional region.

Warping (DTW) [34]. The second one we propose is the LB-Keogh Dynamic Threshold Time Warping (LB-Keogh DTTW) algorithm, which can eliminate some unnecessary map matching precedure in radio maps and dynamically select the threshold and improve the localization accuracy and also improve the performances of the system. In our experiments with only 2 distant deployed TelosB [35] sensors, we find that the average localization error of our BEYOND RSS system outperforms the pure-RSS based approach by 15.19%.

The main contributions of this paper are as follows.

1. We introduced PRR and SNR instead of pure RSS in transceiver-free localization. To the best of our knowledge, we are among the first group to comprehensively utilize both PRR and SNR in the localization system. Moreover, SNR is better than pure RSS to alleviate the noise behavior in the environments and more sensitive to the target.

2. Our proposed algorithms in the BEYOND RSS system can achieve accurate localization results without additional hardware support when the RSS is very weak or the link quality is unstable. Therefore, it is suitable to be applied in sparse environments or in complicated environments with unstable link quality.

3. The empirical analysis considered in this paper is subject to real experiments. We conducted experiments in different complicated indoor environments to verify the applicability of our BEYOND RSS system.

The rest of this paper is organized as follows. In the next section, we describe the related work. In the methodology section, we introduce the basic idea and our two localization algorithms. The proposed scheme with experimental evaluations is validated in Section 4. In the Discussion section, we mainly discuss some key issues to be considered in localization. We finally draw conclusions and propose future work in Section 7.

2 RELATED WORK

Indoor localization basically can be classified into two categories: transceiver-based and transceiver-free.

2.1 Transceiver-based Technologies

Transceiver-based localization requires target to carry a device (e.g., smart phones or smart watches) and some reference nodes deployed in advance. These technologies usually utilize the received signal between the target device and the reference nodes, to localize target. various technologies are proposed in such research area.

Some technologies leverage models to calculate the distance among nodes then localize the target. For example, Time-of-Arrival (TOA) [36] [2] and Time-Difference-of-Arrival(TDOA) technologies can estimated the distance between a pair of transmitter and receiver nodes by measuring the signal propagation time. Angle-of-Arrival (AoA) [37] [1] used the angle of arrival of the signal to the equipment by using the triangulation technique. Antenna array usually is required in such technologies. Some other approaches use Received Signal Strength (RSS) [38] or Channel State Information(CSI) [39] in localization. Usually a radio map is required, and many machine learning and deep learning algorithms are used in localization [40] [41].

Moreover, many useful theories are proposed to improve the localization results. For example, cooperative behavior among nodes are considered in localization [42]. Equivalent Fisher Information (EFI) analysis [43] is developed to determine the basic limits of Network Localization and Navigation (NLN) in localization. Mercury system [44] proposed a real-time belief propagation algorithm to achieve precise positioning. Many multi-target tracking methods [45] are also proposed. A network of radio sensors used for accurate indoor localization and tracking is discussed in detail in Reference [46]. Many methods to improve the system reliability and efficiency are also proposed [47] [48].

2.2 Transceiver-free Technologies

Transceiver-free object localization usually utilizes two following resources: Radio Signal Strength (RSS) and Channel State Information (CSI) [3]–[12]. [3] proposed a novel deep-learning-based indoor fingerprinting system using channel state information (CSI). RSSI Geography Weighted Regression (RGWR) is proposed to solve the fingerprinting database construction problem [5]. However, CSI information is obtained from physical layer information. It is not available for most common devices.

RSS information is easily obtained from common devices, causing it popular in localization. Most RSS-based localization methods require dense deployment of the reference nodes, to avoid environmental influence on the signal. RASS system [14] deployed many sensor nodes on the ceiling as a regular triangle. In each such triangular area, RASS utilized Support Vector Regression (SVR) model to locate transceiver-free object. The work by (J. Wang et al., 2013) proposed a Bayesian Grid Approach (BGA) to locate the target, which is suitable for resource-limited applications. The number of nodes they needed in an area of $8m \times 8m$ is 17 [15]. The work by (G. Yao et al., 2015) could mitigate the

(a) The experimental environment 1.

(b) The experimental environment 2 (target area covers different rooms).
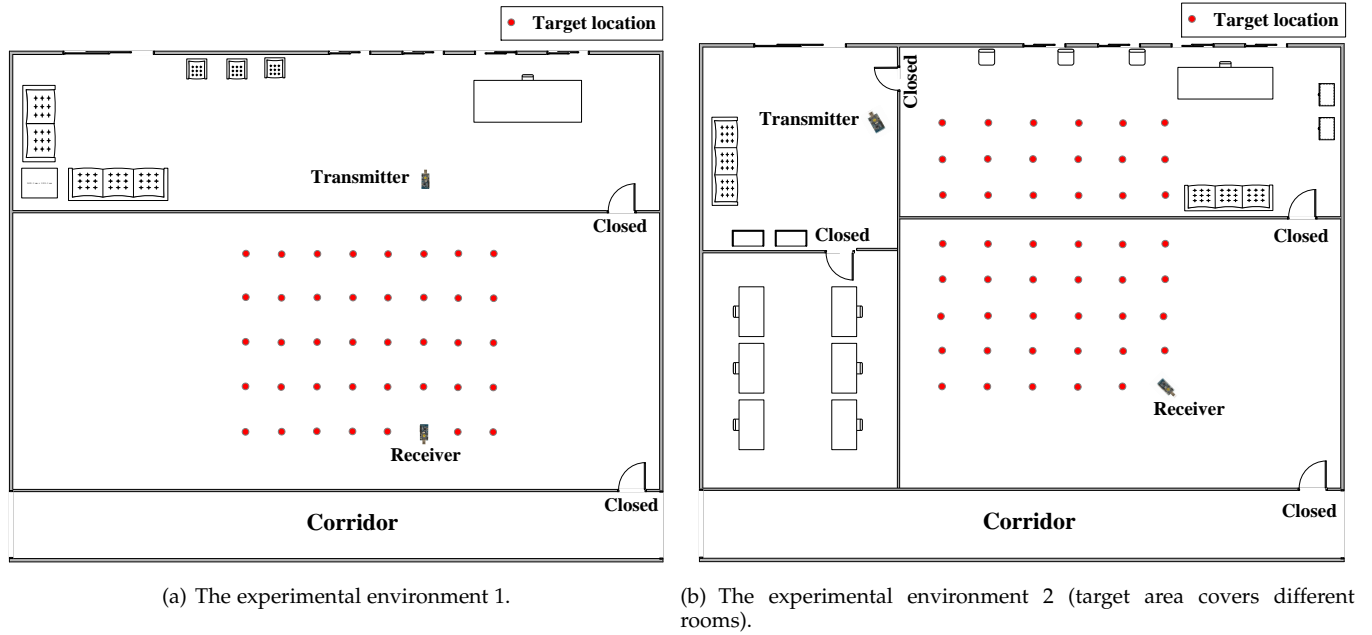
Fig. 4: The experimental environment 1 and 2.

multipath interferences by using the Exponential-Rayleigh (ER) model [16]. At least 17 sensors were required in the above experiment. By and large, the traditional transceiver-free indoor localization methods require at least 3 communication nodes in an experimental area [14]. Tsui, Arvin Wen and Chuang [49] proposed an unsupervised learning method to automatically solve the hardware variance problem in WiFi localization. However, this method is still not suitable for spare networks. The work by (Y. Liu et al., 2012) [50] could monitor and localize the transceiver-free target by using Radio Frequency Identification (RFID) technologies. They also require dense deployment of the tags with $1m$ apart. The work by (Y. Luo et al., 2016) [51] built a hierarchical model to refine the RSS by utilizing Exponential-Rayleigh model and the diffraction-based model. The work by (A. Zanella et al., 2016) [52] also summarized current RSS ranging approaches. The work by (S. Tomic et al., 2017) [53] put forward a distributed target localization through using RSS and Angle-of-Arrival (AOA). There are a large number of RSS improvement approaches [54] [55] [56] [57] [58] based on fingerprinting technologies. But if in a sparsely deployed network, their accuracy decreases dramatically. The work by (C. Liu et al., 2016) [59] proposed a distributed localization approach for device-free target without dense deployment. But it is still not suitable for sparse networks. Zhu [18] proposed to use PRR to assist indoor positioning, but in real environments, the receiver may be affected by the surrounding environment while receiving signals. In addition, we do not rule out that when the packet acceptance rate is 0 during the experiment, we can use NF to locate the auxiliary RSS.

On the other hand, there are some localization aiming to localize the target in sparse wireless networks. CALL System [19] grouped the wireless nodes into component, is able to localized node using the least information. TDL [20] utilized compressive sensing technology to localized
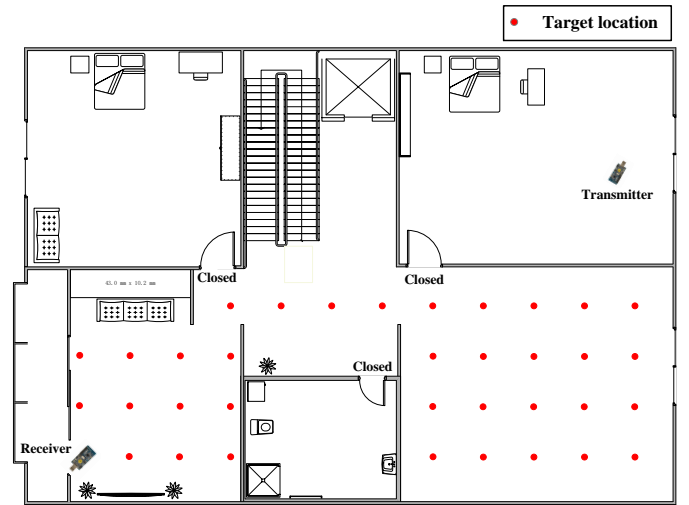
Fig. 5: The experimental environment 3 (a complicated indoor environment).

the moving target. Ghost [21] placed virtual node around the target to create different Voronoi diagrams, so that it can track the target in a sparse wireless network. However, they all require the target to carry a device. DFLAR [22] is able to automatically learn features from the wireless signals, then it used deep learning approach to localize the device-free target and recognize the target gesture. But its wireless network deployment is not very sparse. They deployed 8 nodes in a $7.2m \times 7.2m$ area, while our system only requires 2 nodes in a $5m \times 7m$ area, which is much sparser than their deployment. Specifically, our system works better when the link quality becomes unstable.

Besides, there are also some hybrid systems utilizing

other resource in localization. In 2012, the work by (S. Holm 2012) proposed an ultrasound RSS-based hybrid system for indoor positioning [23]. However, it covers a limited area due to the inherent ultrasound characteristic. The work by (U. L. Yong et al., 2013) combined Visible Light Communication (VLC) with Zigbee signal in localization [24]. The work by (Y. Geng and K. Pahlavan, 2016) applied RF-based and image processing based hybrid system into 3-dimensional localization [25] [27]. The work by (M. A. Bitew et al., 2015) proposed a hybrid localization method by utilizing radio frequency and pyroelectric infrared sensors [26]. The work by (Z. Xiong et al., 2013) jointly utilized Wireless Sensor Network (WSN) and RFID technologies to positioning and tracking target at indoor environment [60]. The work by (H. Cho et al., 2016) [61] combined RSS with the Inertial Measurement Unit (IMU) sensor to reduce the accumulated location error. All these above systems usually require additional hardware support. The work by (X. Huang et al., 2017) [29] used PRR to recognize human motion, but localization can not be realized.

3 METHODOLOGY

In this section, we first give the preliminary and basic idea of how PRR can help RSS-based localization and SNR can improve traditional RSS-based localization, then present the detailed algorithms that we use to localize the target transceiver-free object.

3.1 Preliminary

Transceiver-free localization: In transceiver-free localization, usually a number of reference nodes will be deployed, each reference node will act as a transmitter, or a receiver, or both. Therefore, there are many Transmitter-Receiver (T-R) links in the environment. If no target is around, the received signal of each T-R link is relative stable. On the other hand, if the target appears, the received signals of some T-R links may vary. Such influenced T-R links are usually clustered around the target. The following equation [62], [63] describe such phenomenon.

$$P_{obj} = \frac{P_t G_t G_r \lambda^2 \sigma}{(4\pi)^3 r_1^2 r_2^2} \qquad (1)$$

where r_1 is the distance from the transmitter to the target object, r_2 is the distance from the target object to the receiver, and σ is the radar cross section of the target object. The radar cross section σ is defined as the ratio of scattered power to incident power density.

Therefore, these technologies usually leverage such variance affected by the target and the positions of the influenced T-R links to calculate the target position.

Transition region: In theory, RSS will fade with distance and radio link quality estimation has a fundamental impact on the network performance [64] [65].

When the distance between nodes is not large, usually the PRR is stabilized at 100% (link quality is stable). But when the distance grows larger, the RSS becomes very weak while the link still connects (unstable link quality). In such a situation, the PRR value may vary, which is known as the transition region [30], as shown in Figure 3.

In the transition region, usually the PRR is more sensitive than RSS and shows a larger fluctuation range. We observe from Figure 1 and Figure 2, no matter the target appears or not, the PRR has a larger fluctuation range than RSS. You may see the difference between Figure 1 (a) and Figure 1 (b), Figure 2 (a) and Figure 2 (b), respectively.

Signal-to-Noise Ratio (SNR): Since usually there is a lot of noise in the real world environment, the Noise Floor (NF) will also affect the received signals, causing such a factor not to be negligible. SNR can be calculated as follows [66].

$$SNR = \frac{P_{signal}}{P_{noise}} \qquad (2)$$

where P_{signal} is power of a signal (meaningful input), and P_{noise} is the power of background noise (meaningless or unwanted input).

3.2 Basic Idea

Traditional RSS-based transceiver-free localization technologies usually deploys a number of reference nodes in advance, then leverages the RSS variance affected by the target to calculate the target position. However, we find that, besides RSS, the PRR of some wireless links will also be affected by the target. Especially in those scenarios where the reference nodes are sparsely deployed or having no Line-of-Sight (LoS) paths among reference nodes, this phenomenon is more prominent. Moreover, SNR considers more about the environmental noise. Therefore, instead of traditional pure RSS to localize target nodes, PRR and SNR can together play a constructive role in the localization.

An example is shown below to further explain our basic idea. We deployed two wireless nodes in an indoor environment. One is the transmitter and the other is the receiver. The beacon interval for the transmitter is $15ms$. We arranged them in a Non-Line-of-Sight (NLoS) environment (the two nodes are separated by a wall), which means no LoS path exists between the transmitter and receiver. We observe that, when in a static environment having no transceiver-free target, both PRR and RSS are stable, as Figure 2 shows. Each time window in Figure 2 and Figure 3 is a time period (here is $0.75s$) during which we receive 50 received packets and calculate a PRR. However, when a transceiver-free target object appeared, both PRR and RSS will change, but differently, as shown in Figure 3. In our example, the RSS has small changes while PRR information has prominent changes. In this scenario, PRR is more sensitive to the target. Furthermore, we find that in both environments with and without the target, the NF always occurs differently. So taking both RSS and NF into account (e.g., the SNR can be calculated based on them) may improve the result.

Therefore, it is feasible for us to utilize both PRR and SNR to help RSS-based localization.

3.3 Map Construction

Before introducing our algorithm in detail, we define the location space L as a set of n locations on the ground (assume in a $2D$ area). L is denoted as

$$L = \{l_1 = (x_1, y_1), \cdots, l_n = (x_n, y_n)\} \qquad (3)$$

TABLE 1: Notations used in this paper

Notation	Description
$l_i = (x_i, y_i)$	One transceiver-free target location on the ground
r	Total number of received packets
s	Number of received packets to compute one PRR value
q	Number of PRR values to calculate the target position
K	Number of nearest neighbors
γ	Vector length
T_i^k	The kth data of the vector for the ith location (store the radio map in the offline phase)
P^k	The kth data of the vector (received data) in the online phase
Seq_k	The sequence number of testing point
T_h	The smallest distance between vectors (called the threshold) in the offline state
N_T	Number of reference locations whose vector distances are smaller than the threshold and larger than 0
(x_t, y_t)	The coordinate of the target location
$D(P^\gamma, T_i^\gamma)$	The vector distance between P^K and each T_i^K
n	The number of locations on the map

Fig. 6: Beyond RSS system flow.

where each tuple (x_i, y_i), $1 \leqq i \leqq n$, represents one transceiver-free target location on the ground.

During the offline phase, we arrange a person to represent the transceiver-free target to stand on each location on the ground to build a map which stores the PRR and RSS and the NF value from the receiver, then leverage RSS and NF to calculate SNR value [67] during a fixed time period $\triangle H$ for each pair of transmitter and receiver.

During each fixed time period $\triangle H$, let r be the total number of received packets. We calculate a PRR and a SNR (based on the received average RSS and average NF information), for each s number of packets ($1 < s \leqq r$). Therefore, we will have $q = \lceil r/s \rfloor$ number of SNR value, and that the same number of PRR values as well.

In total, we will have $U = 2q$ number of PRR and SNR values.

Suppose there are M pairs of transmitters and receivers (also referred to as wireless links, we regard the symmetric links as one link) in the environment, we will have $\gamma = M \times U$ number of PRR and SNR values. We can utilize a vector to define it as $T_i^\gamma (1 \leq i \leq n)$.

3.4 Dynamic Time Warping

In this subsection, we will introduce our localization algorithm using Dynamic Time Warping(DTW) [34]. This algorithm is usually used in time series analysis. Since PRR is collected over time, it potentially contains temporal information. We utilize this algorithm in localization.

When the target transceiver-free object appears, for each fixed time period $\triangle H$, we obtain the PRR and the SNR vector P^γ. Then we use DTW algorithm to calculate the vector distance between P^γ and each T_i^γ ($1 \leqq i \leqq n$). The calculation procedure is listed as follows.

At first, the initial value for each $D(P^j, T_i^k)$ is defined as.

$$D(P^j, T_i^k) = \begin{cases} 0 & j = 1 \text{ and } k = 1 \\ +\infty & 1 < j, k \leqq \gamma \end{cases} \quad (4)$$
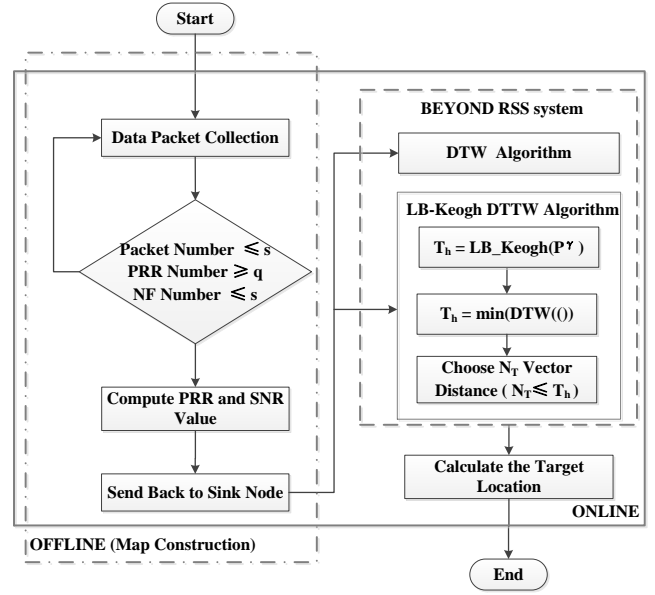
Then we use the following equation to calculate the distance between P^γ and each T_i^γ. when j is larger than 1 or k is larger than 1.

$$D(P^j, T_i^k) = |P^j - T_i^k| + \min \begin{bmatrix} D(P^{j-1}, T_i^k), \\ D(P^j, T_i^{k-1}), \\ D(P^{j-1}, T_i^{k-1}) \end{bmatrix} \quad (5)$$

where P^j represents the j-th feature in the position vector in the online state, and T_i^k represents the k-th feature in the i-th position vector in the map in the offline state. For a total n number of points on the ground, we define a vector Dist to store the n points distance $D(P^j, T_i^\gamma)$ which is calculated by the above equation.

$$Dist_i = D(P^\gamma, T_i^\gamma), \quad 1 \leqq i \leqq n \quad (6)$$

At Last, we choose K number of locations $(x_{c1}, y_{c1}), \cdots (x_{cK}, y_{cK})$ from L, which have smallest $Dist$ values. The coordinate of the target location (X_t, Y_t) can be calculated as

$$X_t = \frac{1}{K} \sum_{i=1}^{K} x_{ci}, \quad Y_t = \frac{1}{K} \sum_{i=1}^{K} y_{ci} \quad (7)$$

The detailed procedure is shown in the DTW algorithm. The time complexity of this algorithm mainly depends on the value of n, namely $O(n^2)$.

3.5 LB-Keogh Dynamic Threshold Time Warping

In this subsection, we propose LB-Keogh Dynamic Threshold Time Warping (LB-Keogh DTTW), which the utilizes LB-Keogh algorithm [68] to efficiently eliminate some unnecessary map matching in the map, and introduce a dynamic threshold in DTW algorithm. It improves the performances of the system. The calculation procedure is listed as follows.
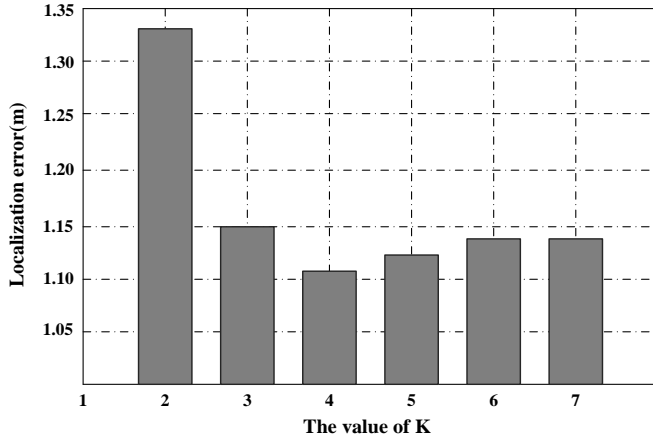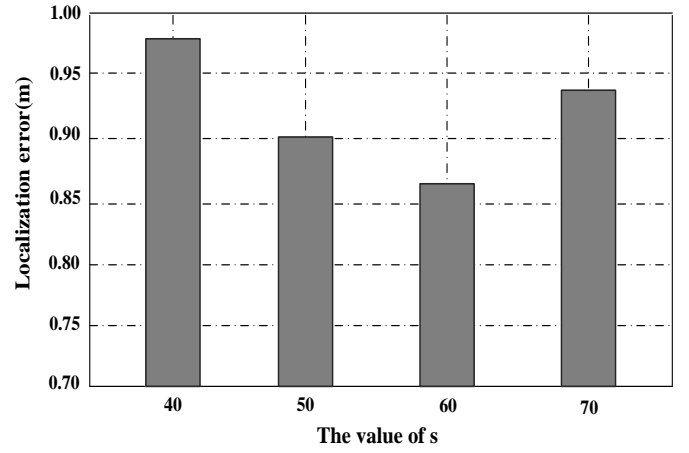
Fig. 7: Impact of the value of K.
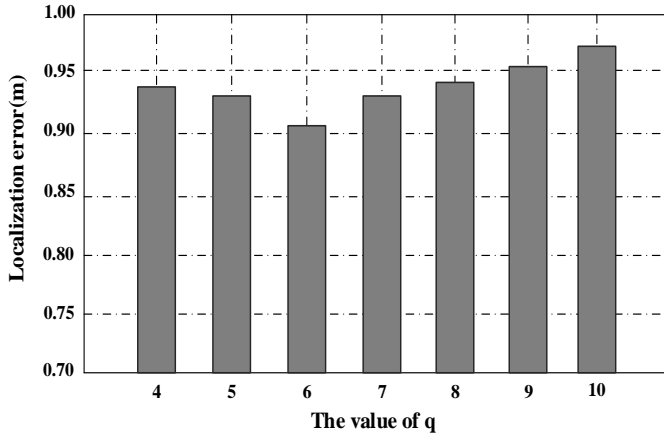

Fig. 9: Impact of the value of s.

Fig. 8: Impact of the value of q.

During the online phase, when the target transceiver-free object comes into the environment, we obtain the PRR and SNR vector P^γ. As shown in Figure 10. At first, we will calculate the upper and lower bounds of the vector P^γ (P^γ include all P^j), each maximum and minimal value of the feature P^j is defined as:

$$P_{max}^j = max(P^{j-w}, P^{j-w+1}..., P^j, P^{j+1}, ..., P^{j+w})$$
$$P_{min}^j = min(P^{j-w}, P^{j-w+1}..., P^j, P^{j+1}, ..., P^{j+w}) \quad (8)$$
$$(w \leqq j \leqq \gamma - w)$$

where w is a sliding window length. P_{max}^j, P_{min}^j represents the maximum and minimal value of the j-th of the vector P^γ respectively.

Second, we will calculate each LB-Keogh distance between P^γ and each vector T_i^γ ($1 \leqq i \leqq n$) in the map through the LB-Keogh algorithm. The LB-Keogh distance between them is shown in the gray in Figure 10. The LB-Keogh distance is defined as:

$$LB_i(P^\gamma, T_i^\gamma) = \sqrt{\sum_{j=1}^{\gamma} \begin{cases} (T_i^j - P_{max}^j)^2 & P_{max}^j \leq T_i^j \\ (T_i^j - P_{min}^j)^2 & T_i^j \leq P_{min}^j \\ 0 & otherwise \end{cases}}$$
$$(1 \leqq i \leqq n) \quad (9)$$

Then, we gets the smallest LB-Keogh distance LB^{min}. LB^{min} is defined as:

$$LB^{min} = min(LB_1(P^\gamma, T_1^\gamma), ..., LB_i(P^\gamma, T_i^\gamma), \\ ..., LB_n(P^\gamma, T_n^\gamma)) \quad (10)$$

Third, we defined a set Q to get the vectors which LB-Keogh distance equal LB^{min}. Importantly, the number of elements in the Q is more than 0 and less than n. The set Q is defined as:

$$Q = \{T_x^\gamma \mid x \in \{1, 2, ..., n\} \cup LB_x(P^\gamma, T_x^\gamma) = LB^{min}\} \quad (11)$$

The detailed procedure is shown in the Pseudocode of the LB-Keogh distance Algorithm.

However, we defined q represents the number of elements in the Q. When q is more than 1, we will use the Dynamic Threshold Time Warping(DTTW) to calculate the vector distance between P^γ and each T_x^γ in the set Q.

At first, for any pair of vector T_u^γ and T_v^γ ($T_u^\gamma \in Q$, $T_v^\gamma \in Q$), we calculate their distance $Dist_{u \times v}$ as follows.

$$Dist_{u \times v} = D(T_u^\gamma, T_v^\gamma) \quad (12)$$

here, the vector distance is calculated using the DTW algorithm introduced in the last subsection. Then, we define threshold T_h as the smallest vector distance which is not equal to 0 in the calculation results.

$$T_h = min(Dist_1, Dist_2, ...Dist_{u \times v}) \quad (13)$$

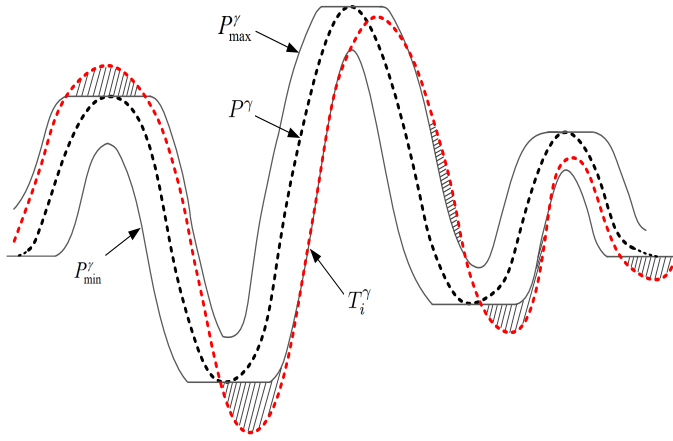Then we define N_T as the number of reference locations whose vector distances are smaller than the threshold, in

Fig. 10: The black dotted line represents the vector P^γ, and the red dotted line represents the T_i^γ. The vectors P_{max}^γ and P_{min}^γ represents the upper and lower bound of P^γ respectively.

Algorithm DTW algorithm

Require: The PRR and SNR sequence: P^γ
    The training map is stored in T_n^γ
Ensure: the object location (X_t, Y_t)
 1: **for** $i \leftarrow 1$ to n **do**
 2:    $Dist_i \leftarrow DTW(P^\gamma, T_i^\gamma)$;
 3: **end for**
 4: **for** $k \leftarrow 1$ to n **do**
 5:    $Seq_k = k$;
 6: **end for**
 7: **for** $k \leftarrow 1$ to n **do**
 8:    **for** $j \leftarrow k+1$ to n **do**
 9:      **if** $Dist_k > Dist_j$ **then**
10:       $tem \leftarrow Dist_k; Dist_k \leftarrow Dist_j; Dist_j \leftarrow tem$;
11:       $temp \leftarrow Seq_k; Seq_k \leftarrow Seq_j; Seq_j \leftarrow temp$;
12:      **end if**
13:    **end for**
14: **end for**
15: $X_{Sum} = 0, Y_{Sum} = 0, a = 0$;
16: **for** $i \leftarrow 1$ to K **do**
17:    $X_{Sum} \leftarrow X_{Sum} + X_{Seq_i}$;
18:    $Y_{Sum} \leftarrow Y_{Sum} + Y_{Seq_i}; a \leftarrow K$;
19: **end for**
20: $X_t \leftarrow \frac{1}{a}X_{Sum}; Y_t \leftarrow \frac{1}{a}Y_{Sum}$;

---

the target location estimation. When N_T is larger than 0, the value of K is equal to N_T. However, if all the vector distances are larger than the threshold ($N_T = 0$), we will use a fixed K value K_{fix} instead (how to choose this value will be discussed in the latter subsection). The calculation procedure is as follows.

$$K = \begin{cases} N_T & 0 < N_T \\ \\ K_{fix} & N_T = 0 \end{cases} \quad (14)$$

At last, the coordinate of the target location (X_t, Y_t) can

---

Algorithm LB-Keogh distance algorithm

Require: The PRR and SNR sequence: P^γ
    One point of the training map T_i^γ
    The sliding window distance w
Ensure: the LB-Keogh distance $LB_{distance}$ of i-th in the map
 1: $LB_{distance} \leftarrow 0$;
 2: **for** $ind \leftarrow 1$ to $len(P^\gamma)$ **do**
 3:    $P_{max}^{ind} \leftarrow P^{ind}$
 4:    $P_{min}^{ind} \leftarrow P^{ind}$
 5:    **if** $0 \leqq (ind - w)$ **and** $(ind + w) \leqq len(P^\gamma)$ **then**
 6:      **for** $c \leftarrow ind - w$ to $ind + w$ **do**
 7:       $P_{max}^{ind} \leftarrow max(P^c, P_{max}^{ind})$;
 8:       $P_{min}^{ind} \leftarrow min(P^c, P_{max}^{ind})$;
 9:      **end for**
10:    **end if**
11:    **if** $(ind - w) \leqq 0$ **then**
12:      **for** $c \leftarrow 1$ to $ind + w$ **do**
13:       $P_{max}^{ind} \leftarrow max(P^c, P_{max}^{ind})$;
14:       $P_{min}^{ind} \leftarrow min(P^c, P_{max}^{ind})$;
15:      **end for**
16:    **end if**
17:    **if** $len(P^\gamma) \leqq (ind + w)$ **then**
18:      **for** $c \leftarrow ind - w$ to $len(P^\gamma)$ **do**
19:       $P_{max}^{ind} \leftarrow max(P^c, P_{max}^{ind})$;
20:       $P_{min}^{ind} \leftarrow min(P^c, P_{max}^{ind})$;
21:      **end for**
22:    **end if**
23:    **if** $P_{max}^{ind} \leqq T_i^{ind}$ **then**
24:      $LB_{distance} \leftarrow LB_{distance} + (T_i^{ind} - P_{max}^{ind})^2$;
25:    **end if**
26:    **if** $T_i^{ind} \leqq P_{min}^{ind}$ **then**
27:      $LB_{distance} \leftarrow LB_{distance} + (T_i^{ind} - P_{min}^{ind})^2$;
28:    **end if**
29: **end for**
30: **return** $sqrt(LB_{distance})$;

---

be calculated as

$$(X_t, Y_t) = \frac{1}{K} \sum_{i=1}^{K} (x_{ci}, y_{ci}) \quad (15)$$

The detailed procedure is shown in the localization algorithm of LB-Keogh DTTW. The time complexity of this algorithm mainly depends on the value of n and p, namely $O(p * n)$.

Some important notations used in this paper are listed in the Table 1.

4 EXPERIMENT

4.1 Experiment Setting & System Flow

The experiment was conducted in three different indoor environments. The experimental environment 1 is $5m \times 8m$, and all sample targets are deployed in one indoor room. The experimental environment 2 is $6m \times 8m$, in which 18 target samples are deployed in the first indoor room, and the other 30 target samples are deployed in the second indoor room. The experimental environment 3 includes two sub-room ($5m \times 4m$ and $3m \times 2m$ respectively) and one corridor
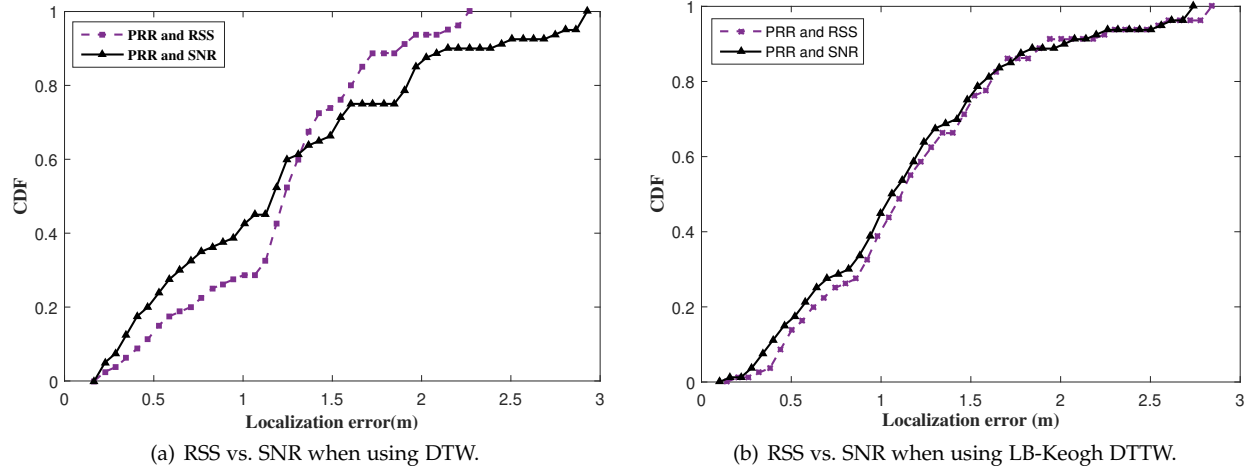
(a) RSS vs. SNR when using DTW.

(b) RSS vs. SNR when using LB-Keogh DTTW.

Fig. 11: Impact of SNR in environment 1.

(a) RSS vs. SNR when using DTW.

(b) RSS vs. SNR when using LB-Keogh DTTW.
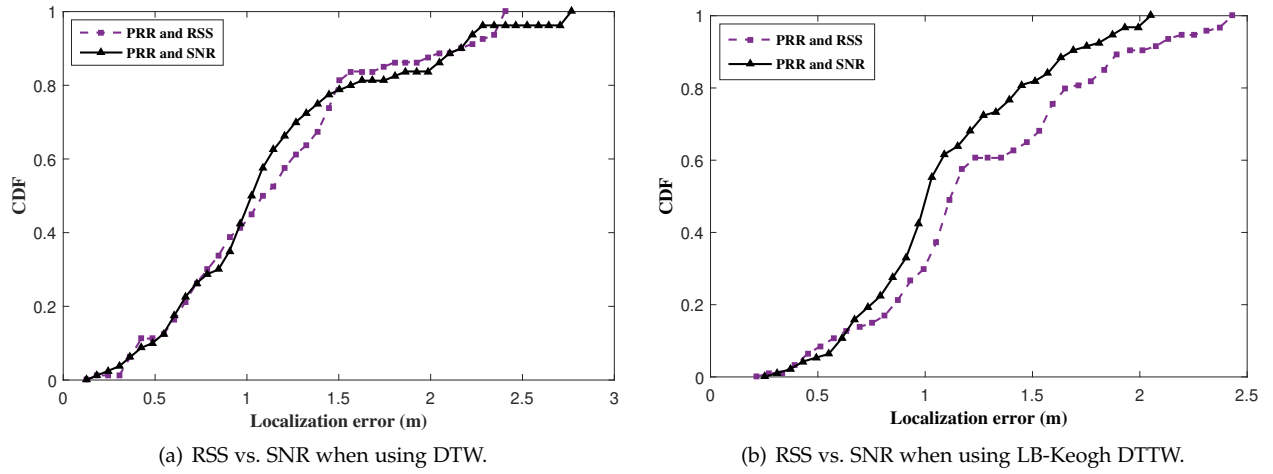
Fig. 12: Impact of SNR in environment 2.

(a) RSS vs. SNR when using DTW.

(b) RSS vs. SNR when using LB-Keogh DTTW.
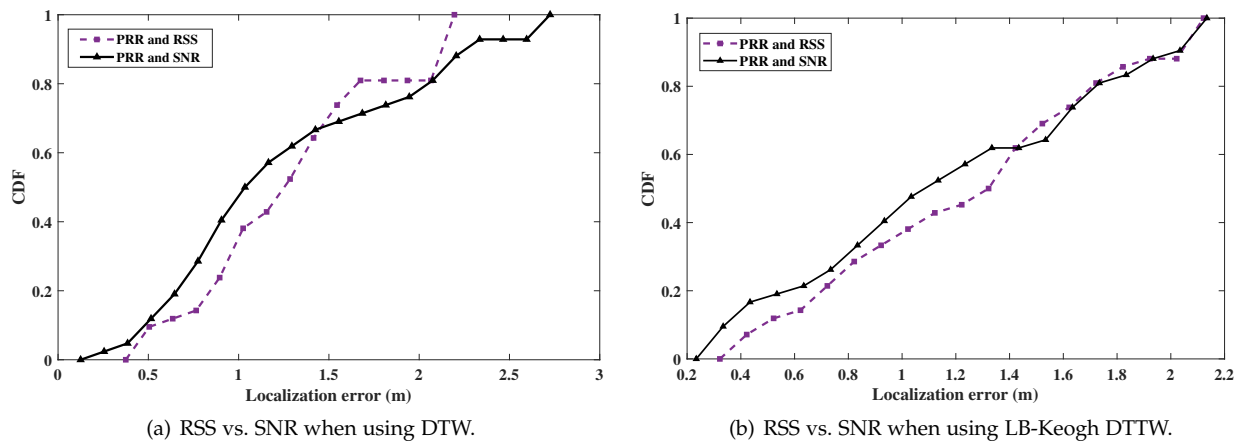
Fig. 13: Impact of SNR in environment 3.

$(3m \times 1m)$. This scenario is more complicated than the previous two scenarios since it involved the two different rooms which are separated by the other room and a corridor area as well. All red points represents the sample target in the map, as shown in Figure 4 (a), (b) and Figure 5. In our experiment, we set up the sparse deployment by only using two nodes. They are two popular TelosB sensor nodes [35] deployed and separated by a wall. However, the difference between

(a) Localization error in environment 1.

(b) Localization error in environment 2.

(c) Localization error in environment 3.

Fig. 14: Algorithm results based on all sample target positions.

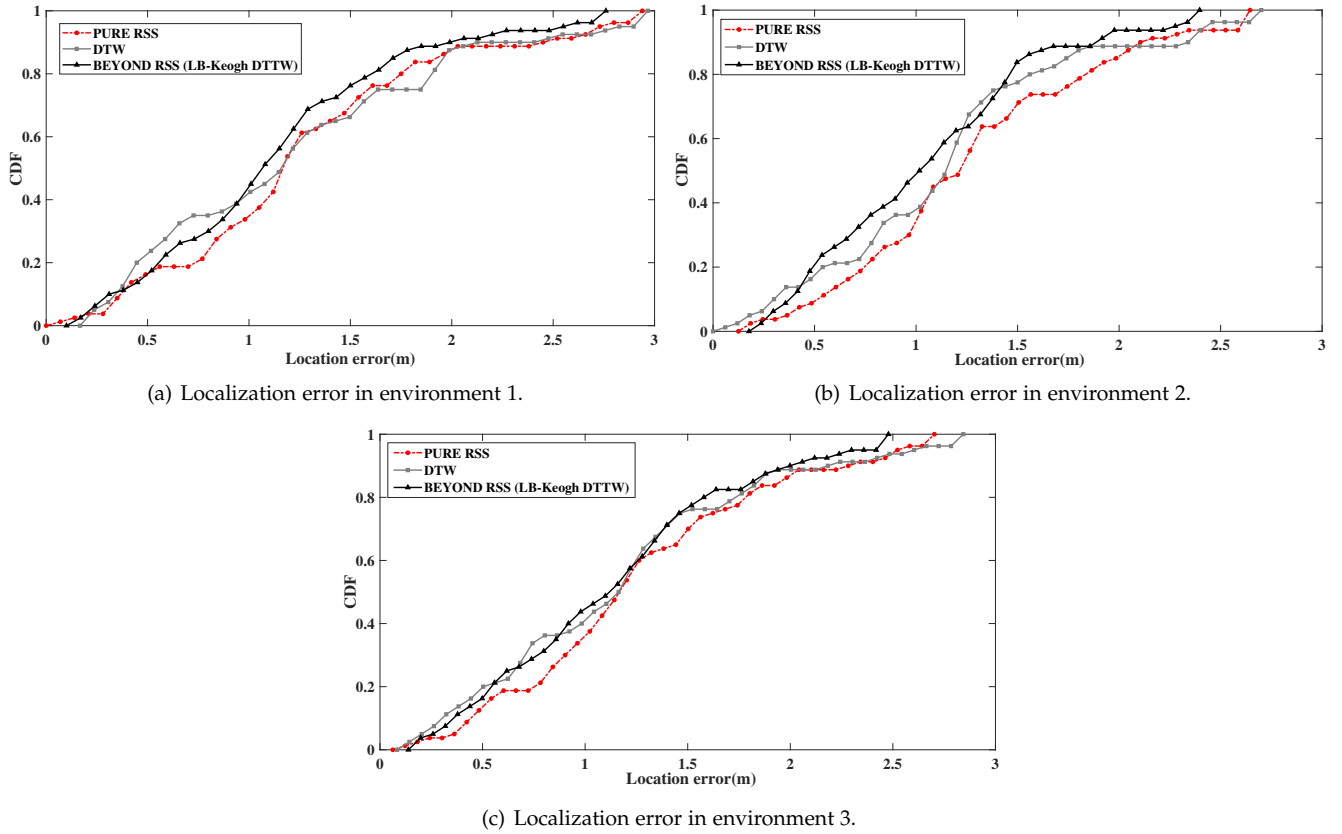three experimental environments is that the transmitter and receiver in the experimental environment 1 are placed in a straight line, while the transmitter and receiver in the experimental environment 2 and 3 are placed diagonally. TelosB is a low power radio device. One sensor acts as the transmitter while the other acts as the receiver. Therefore, there exists no LoS signal path between them. The default transmission power is set as $-25dBm$ (power level 3) and the radio frequency is $2.4GHz$. The beacon interval of the transmitter has been defaulted at $15ms$. The data received by the transceiver will be transmitted to our server for processing.

Our BEYOND RSS system flow chart is described in Figure 6. At first during the training phase, for each target location on the ground, we collect the received packets. Each receiver will compute the PRR value and the SNR after receiving every s (in our experiment this value is default at 50) packets, then send back to the sink along with RSS and NF information. Therefore, the SNR value can be calculated based on the received RSS and NF information. After we get q (in our experiment this value is set to default at 6) number of PRR values, the collection procedure is completed and the map is then constructed. We will discuss how to set the parameters of s and q in the later subsection of this paper.

Second, during the online phase, when the transceiver-free target appears in the environment, similarly, each receiver will also collect the received packets. Then, we compute the PRR value accordingly. At the same time, RSS and NF information will also be sent back to the sink, for every s

packets the SNR is computed based on the average RSS and average NF. After we get q number of PRR values, users can choose KNN, DTW or LB-Keogh DTTW to calculate the target localization. When the procedure repeats, we can track the target transceiver-free object.

4.2 Impact of values K

In this subsection, we investigate how the value of K will affect the localization error.

In our experiment, we test different values of K from 2 to 7, as shown in Figure 7. We find that the localization error is smallest when the value of K is set to 4. If the value of K is smaller than 4 or larger than 4, the localization error is larger.

The reason is as follows: if the K is lower than 4, the number of nearest neighbors may be too less. Therefore, if some neighbors are far away from the real target position due to the interference, then their impact on the localization error can be enlarged. On the contrary, if the K is larger than 4, it will lead to fuzzy classification.

Therefore, in our later experiment, we choose the value of K as 4 by default.

4.3 Impact of Parameter q

The value of q depends upon how many PRR values are considered to calculate the target location. It decides the input vector dimension and is one of the key parameters to the performance of our system. If this value is set very

(a) Localization error in environment 1.

(b) Localization error in environment 2.
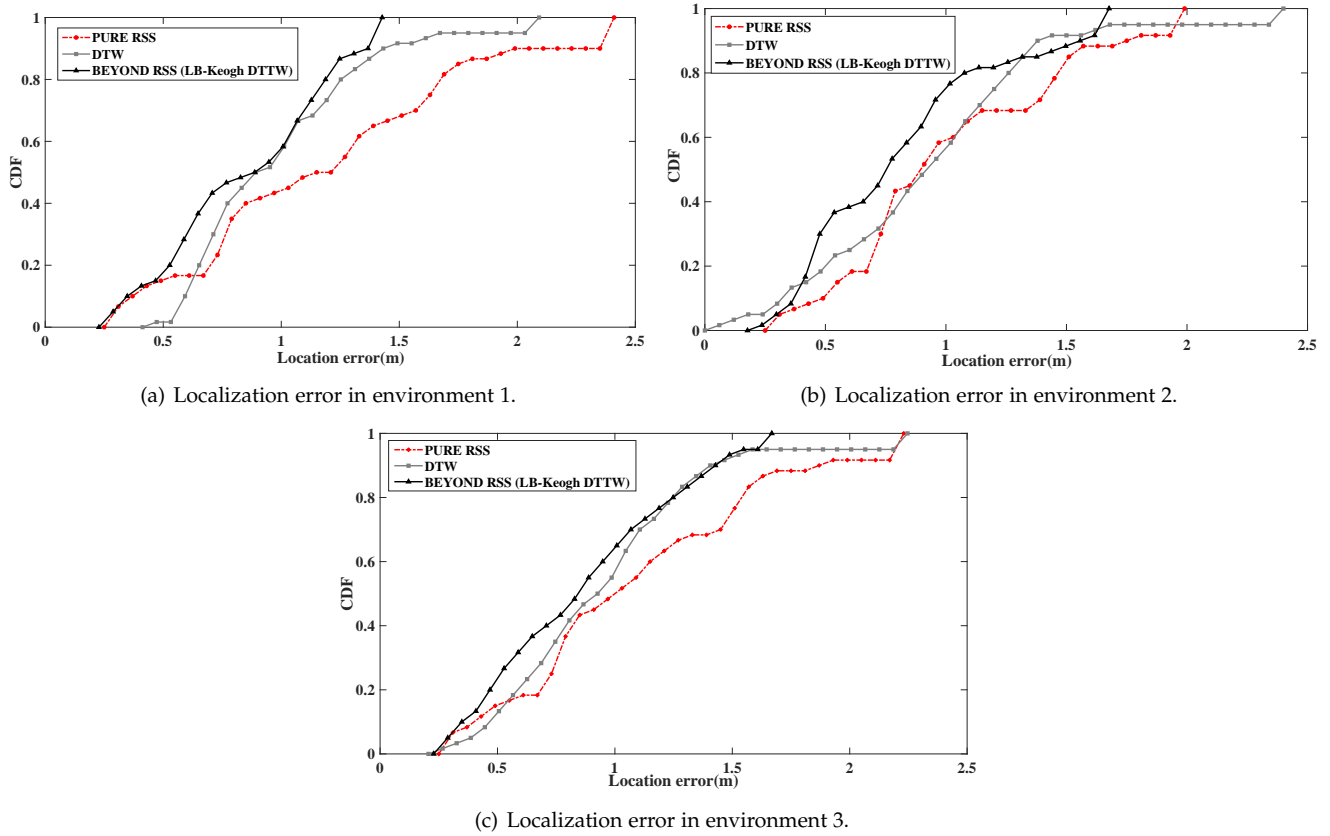

(c) Localization error in environment 3.

Fig. 15: Algorithm results based on non-border sample target positions.

large, the time required to collect the packets will be longer, resulting in a high system delay. On the contrary, if this value is set too small, the localization error will be affected.

In order to test how the value of q will impact the localization error, we test different values of q from 4 to 10 (the other parameter s is randomly chosen), as shown in Figure 8. We find that the localization error is smallest when the value of q is set to 6. For the other values of q smaller than 6 or larger than 6, the localization error is larger. The reason can be attributed to the following: if the q is lower than 6, the time is too short to get enough PRR values for the localization algorithm. On the contrary, if the q is set higher, the time is too long and there is a possibility of introducing noise information in the localization algorithm.

Therefore, in our later experiment, we consciously choose the value of q as 6.

4.4 Impact of Parameter s

The value of s depends on how many packets are required to calculate one PRR value. It is also one of the key parameters which decide the localization error and system performance. If this value is set very large, the time to receive all the required packets will be longer, resulting in a high system delay. On the contrary, if this value is set too small, PRR value may not be well represented.

In order to test how the value of s will impact the localization error, we test different values of s from 40 to 70, in steps of 10, as shown in Figure 9. We find that the localization error is smallest when the value of s is set to 50

or 60, wherein the localization error can reach about $0.9m$. For the values of s smaller than 50, the localization errors are larger. The reason is that, if the value of s is set too low, the time is too short to get a well-represented PRR. For the values of s larger than 60, the localization errors are larger. The reason may be attributed to the following: If we calculate one PRR value based on a large number of received packets, it increases the possibility of introducing more noise information. Moreover, latency will increase.

Therefore, in our later experiment, in order to get a tradeoff between localization error and system latency, we choose the value of s as 50 instead of 60, since 60 will increase the system latency. But this value can be decided by the users depending on their priority.

4.5 Comparison between SNR and RSS

In this subsection, we will investigate how SNR is better than RSS.

In order to comprehensively conduct experimental analysis, we used both DTW and LB-Keogh DTTW in the experiments. In the experimental environment 1, when we only leverage PRR and RSS features, the average localization error is $1.23m$ and $1.16m$ respectively. However, when we leverage PRR and SNR features (use SNR instead of RSS), the average localization error is $1.15m$ and $1.11m$, the Cumulative Distribution Function (CDF) is as shown in (a) and (b) of Figure 11. The average localization accuracy is 6.50% and 4.31% higher than using PRR and RSS, respectively. In the experimental environment 2, when we

Algorithm DTTW localization algorithm

Require: The PRR and SNR sequence: P^γ
  The training map is stored in T_p^γ
Ensure: the object location (X_t, Y_t)
 1: $mini \leftarrow 0$;
 2: **for** $i \leftarrow 1$ to p **do**
 3:   $Dist_i \leftarrow DTW(P^\gamma, T_i^\gamma)$;
 4: **end for**
 5: $mini \leftarrow max(Dist_i)$;
 6: **for** $j \leftarrow 1$ to p **do**
 7:   **for** $k \leftarrow 1$ to p **do**
 8:     $Dist_k \leftarrow DTW(T_j^\gamma, T_k^\gamma)$;
 9:     **if** $Dist_k < mini$ and $Dist_k! = 0$ **then**
10:       $mini \leftarrow Dist_k$;
11:     **end if**
12:   **end for**
13: **end for**
14: $T_h = mini$;
15: **for** $k \leftarrow 1$ to p **do**
16:   $Seq_k = k$;
17: **end for**
18: **for** $k \leftarrow 1$ to p **do**
19:   **for** $j \leftarrow k + 1$ to p **do**
20:     **if** $Dist_k > Dist_j$ **then**
21:       $tem \leftarrow Dist_k; Dist_k \leftarrow Dist_j; Dist_j \leftarrow tem$;
22:       $temp \leftarrow Seq_k; Seq_k \leftarrow Seq_j; Seq_j \leftarrow temp$;
23:     **end if**
24:   **end for**
25: **end for**
26: $X_{Sum} = 0, Y_{Sum} = 0, a = 0$;
27: **for** $i \leftarrow 1$ to $len(Dist_k)$ **do**
28:   **if** $Dist_i < T_h$ **then**
29:     $X_{Sum} \leftarrow X_{Sum} + X_{Seq_i}$;
30:     $Y_{Sum} \leftarrow Y_{Sum} + Y_{Seq_i}; a \leftarrow a + 1$;
31:   **end if**
32:   **if** $Dist_0 > T_h$ **then**
33:     **for** $i \leftarrow 1$ to K **do**
34:       $X_{Sum} \leftarrow X_{Sum} + X_{Seq_i}$;
35:       $Y_{Sum} \leftarrow Y_{Sum} + Y_{Seq_i}$;
36:     **end for**
37:     $a \leftarrow K$;
38:   **end if**
39: **end for**
40: $X_t \leftarrow \frac{1}{a}X_{Sum}; Y_t \leftarrow \frac{1}{a}Y_{Sum}$;

---

only leverage PRR and RSS features, the average localization error is $1.13m$ and $1.10m$ respectively. However, when we leverage PRR and SNR features, the average localization error is $1.11m$ and $1.07m$, as shown in (a) and (b) of Figure 12. The average localization accuracy is 1.77% and 2.73% higher than using PRR and RSS, respectively. In the experimental environment 3, when we only leverage PRR and RSS features, the average localization error is $1.14m$ and $1.11m$ respectively. However, when we leverage PRR and SNR features, the average localization error is $1.10m$ and $1.06m$, as shown in (a) and (b) of Figure 13. The average localization accuracy is 2.51% and 4.50% higher than using PRR and RSS, respectively.

Therefore, no matter which algorithm we choose, we find that the localization accuracy using SNR features is higher than using traditional RSS features.

4.6 Localization Error

In the subsection, we will test the localization error of our BEYOND RSS system (LB-Keogh DTTW) in different environments. Specifically, environment 1 and 2 are two indoor environments which are shown in Figure 4 (a) and (b), respectively. Furthermore, we also test a very complicated indoor environment 3, where the transmitter and receiver are separated in different rooms by various walls, as shown in Figure 5.

For experimental environment 1, in total, we tested 40 target positions on the ground. Among them, there are 10 sample target positions on the border area. For the experimental environment 2, we tested 47 target positions, of which 17 sample target positions are on the border area. For the experimental environment 3, we tested 35 target positions, of which 10 sample target positions are on the border area.

The experiment results are shown in Figure 14 and Figure 15. Figure 14 is the algorithm results based on all sample target positions, while Figure 15 is the algorithm result based on non-border sample target positions.

1. No matter which algorithm we choose, our BEYOND RSS (LB-Keogh DTTW) system always outperforms the pure RSS-based approach in three environments for all the samples. The pure RSS-based localization errors are $1.29m$, $1.27m$ and 1.26, respectively. On the other hand, the localization error of LB-Keogh DTTW can reach $1.11m$, $1.07m$ and 1.06 in the above three environments, respectively. Therefore, our BEYOND RSS system outperforms the pure RSS-based approach by about 13.95% and 15.75% and 15.87% respectively. On average, our BEYOND RSS system outperforms the pure RSS-based approach by about 15.19%.

2. In environment 1, the localization errors of DTW and LB-Keogh DTTW for all the samples are $1.15m$ and $1.11m$, respectively. LB-Keogh DTTW outperforms the DTW by about 3.5%. In environment 2, their localization errors are $1.11m$ and $1.07m$, respectively. LB-Keogh DTTW outperforms the DTW by about 3.60%. In environment 3, their localization errors are $1.10m$ and $1.06m$, respectively. LB-Keogh DTTW outperforms the DTW by about 3.64%. On average, LB-Keogh DTTW outperforms the DTW by about 3.58%.

3. We further compare our algorithms between non-border samples and all the samples in all the environments. we find that the localization error in the non-border area is lower than it in all the areas. For environment 1, 2 and 3, the localization error of our BEYOND RSS (LB-Keogh DTTW) system can reach $0.88m$, $0.81m$ and $0.83m$ respectively for the non-border area, while it can reach around $1.11m, 1.07m$ and 1.06 respectively for all area including the border. The average localization error difference between samples in all the areas and the non-border areas is around 21.51%. Therefore, we have better localization error for the target positions in the non-border area. The reason is possible attributed to the following. In the border area, when we build the map, the number of neighbor locations is too less, so that it will influence the localization results. Such a phenomenon often occurs in the indoor localization approaches [69].
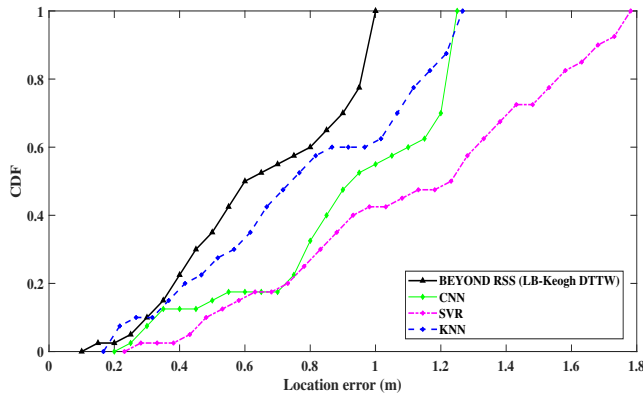
Fig. 16: Algorithm comparison in experimental environment 1.

Fig. 17: Algorithm comparison in experimental environment 2.

In a real application, when users require high accuracy (low localization error), LB-Keogh DTTW is recommended. If users do not want to take the dynamic threshold into consideration, they may skip this step and use DTW instead, but some accuracy may be sacrificed.

4.7 Algorithm Comparison

In this subsection, in order to further investigate the performance of our BEYOND RSS system(LB-Keogh DTTW), we also compare our algorithm with KNN, and the popular machine learning algorithms such as Support vector regression (SVR) [70] and Convolutional Neural Networks (CNN) in deep learning [71].

As shown in Figure 16, Figure 17 and Figure 18, in experiment 1, the localization error of KNN, SVR and CNN algorithm only can reach about $1.16m$, $1.74m$ and $1.33m$, respectively. Similarly, in environment 2, the localization error of the KNN, SVR and CNN algorithm only can reach about $1.18m$, $1.72m$ and $1.32m$, respectively. In addition, in environment 3, the localization error of the KNN, SVR and CNN algorithm only can reach about $1.19m$, $1.49m$ and $1.38m$, respectively. On the contrary, The localization error of our BEYOND RSS system (LB-Keogh DTTW) can reach $0.88m$, $0.81m$ and $0.83m$ respectively. On average, LB-Keogh DTTW outperforms KNN, SVR, CNN by about 21.87%, 50.63% and 38.19% respectively.

The reason why our BEYOND RSS system is more accurate than SVR and CNN is that our data is time-series signals and the data size is small. Therefore, traditional machine learning and deep learning possibility do not show many advantages for a small data set.

5 LATENCY

The latency of our BEYOND RSS system (LB-Keogh DTTW) depends on how long the server (a sink is connected to it) to obtain all the PRR and SNR information. The running time of the localization algorithms on the server can be ignored.

Suppose the beacon interval for the transmitter to transmit a packet to the receiver is T_I in our system, and again the number of collecting packets to compute a PRR value is s, and the number of PRR values to calculate a target position is q, the latency can be calculated as follows.
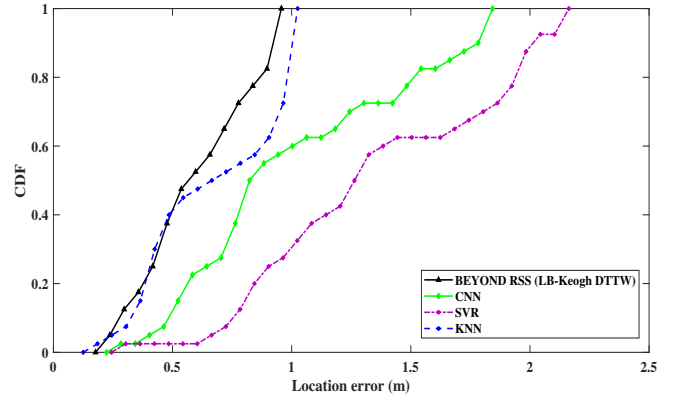
$$T_{latency} = q \times s \times T_I \quad (16)$$

In our system, the value of q is set as 6, the value of s is set as 50, and the beacon interval is set as $15ms$. Therefore, the total latency is $15ms \times 6 \times 50 = 4.5s$.

Although the latency is not very low, it is still a good choice for sparse wireless networks and can reduce the deployment cost. In real scenarios, users may get a tradeoff between system latency and localization to get a tolerated error with lower latency.

6 DISCUSSION

The BEYOND RSS system does not require the target to carry any device (such as smart phones or sensors). Compared with traditional transceiver-free technologies, our BEYOND RSS system has less requirements for the reference node deployment and is able to reduce the deployment cost. It allows very sparse deployment even in a non-line-of-sight deployment. Moreover, BEYOND RSS system imposes minimal assumptions on the environment and the available hardware. We use SNR instead of pure RSS to reduce the impact of noise, making our system more sensitive to the target. Any transceiver with RSS and Noise Floor measurement are employable by BEYOND RSS system.

The potentials and limitations of BEYOND RSS system are discussed in detail as below.

First, in the current localization approaches, there are many features (e.g., RSS, CSI), which are popular in localization. SNR considers more factors than RSS. Furthermore, PRR and SNR are critical features that potentially can help almost all the traditional localization approaches, especially when the nodes are sparsely deployed and the link quality is not that good.

Second, a critical problem of localization approaches is radio interference by the surrounding environments, especially from external radio sources. It may deviate the RSS values and CSI values, and even cause the measurement to fail. In our experiments, we introduce SNR, which can learn how noise behavior interferes with original signals. Thus, it can improve almost all the RF-based localization technologies.

Third, the fingerprinting-based localization is sensitive to the changes of environment. It is a general problem for almost all fingerprinting technologies including ours. Our methods aim to solve another problem, in which when the link quality becomes unstable due to the sparse deployment or object interference in a complex indoor environment, how to utilize PRR and NF to improve the localization performance with low latency.

Fourth, in some other special scenarios where nodes are densely deployed and the link quality is stable, PRR may not vary (e.g., always 100%) during the experiment. In such cases, PRR may not help in localization, while SNR still works and can help in localization. On the other hand, if nodes are deployed in a very dense environment, too many packet transmissions occurring during a limited time period can cause packets collisions [72], or link quality becomes unstable in a complicate indoor environment, PRR is still able to help in localization. The impact of PRR in densely deployed scenarios is left for further investigation.

At last, if Beyond RSS system is applied in a tracking system, it will experience more tracking latency (in our system it is $4.5s$). This may not satisfy those applications which require real-time tracking results. A possible way to reduce the latency is to dynamically adjust the q values. However, it is our first try to localize, using PRR and SNR. In this paper, we proved that PRR and SNR can potentially help almost all the RF-based localization technologies. The experimental results have also shown the feasibility of our proposed system. Further improvement on the latency is left for our future work.

7 CONCLUSION AND FUTURE WORK

In this paper, we propose an approach, which leverages PRR and SNR instead of pure RSS in transceiver-free object localization. Both PRR and SNR can be obtained from a common device without additional hardware costs. Moreover, it is more sensitive to the target and can be widely used in sparse wireless networks or complex noisy indoor environments, where LoS path often does not exist among reference nodes.

We propose two algorithms, which are able to accurately localize the transceiver-free target. LB-Keogh DTTW, which can eliminate some unnecessary map matching precedures in radio maps and dynamically select the threshold, so that the localization accuracy can be improved. In our experiment, we only use two wireless nodes in indoor environments. Our BEYOND RSS system are outperform the pure RSS based approach by about 15.19%. Our approach has the potential to improve almost all the RF-based localization by using common hardware.

As for future work, first, we may perform our experiment in a larger and more complicated indoor environment, where we adopt more reference nodes. Second, reference nodes with different sparse deployment should be tested. In this paper, we have randomly put the reference nodes. We may test different deployments in the future. Third, we may try a different algorithm to get a smaller error and lower latency. These results require further investigation in the future. At last, we will expand the scope of applications making it to work not only in sparse networks but also in a dense deployment.
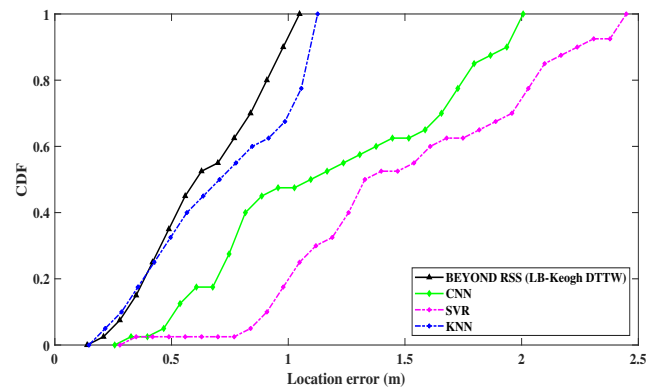

Fig. 18: Algorithm comparision in experimental environment 3.

REFERENCES

[1] M. Kotaru, K. Joshi, D. Bharadia, and S. Katti, "Spotfi: Decimeter level localization using wifi," *Proceedings of the 2015 ACM Conference on Special Interest Group on Data Communication*, pp. 269–282, 2015.

[2] F. Adib, Z. Kabelac, and D. Katabi, "Multi-person localization via {RF} body reflections," *12th {USENIX} Symposium on Networked Systems Design and Implementation ({NSDI} 15)*, pp. 279–292, 2015.

[3] X. Wang, L. Gao, S. Mao, and S. Pandey, "Csi-based fingerprinting for indoor localization: A deep learning approach," *IEEE Transactions on Vehicular Technology*, vol. 66, no. 1, pp. 763–776, Jan 2017.

[4] M. Kotaru, K. Joshi, D. Bharadia, and S. Katti, "Spotfi:decimeter level localization using wifi," *Acm Sigcomm Computer Communication Review*, vol. 45, no. 4, pp. 269–282, 2015.

[5] Y. Du, D. Yang, and C. Xiu, "A novel method for constructing a wifi positioning system with efficient manpower," *Sensors*, vol. 15, no. 4, pp. 8358–8381, 2015. [Online]. Available: http://www.mdpi.com/1424-8220/15/4/8358

[6] C. Yang and H. Shao, "Wifi-based indoor positioning," *IEEE Communications Magazine*, vol. 53, no. 3, pp. 150–157, March 2015.

[7] Z. Xi, L. Wei, J. Lan, Z. Xi, L. Wei, and J. Lan, "Based on the csi regional segmentation indoor localization algorithm," in *Green Energy and Sustainable Development I: International Conference on Green Energy and Sustainable Development*, 2017.

[8] X. Wang, X. Wang, and S. Mao, "Deep convolutional neural networks for indoor localization with csi images," *IEEE Transactions on Network Science and Engineering*, vol. PP, no. 99, pp. 1–1, 2018.

[9] X. Wang, "Resloc: Deep residual sharing learning for indoor localization with csi tensors," *IEEE International Symposium on Personal*, 2017.

[10] P. Yazdanian and V. Pourahmadi, "Deeppos: Deep supervised autoencoder network for csi based indoor localization," 2018.

[11] Q. Gao, W. Jie, X. Ma, X. Feng, H. Wang, Q. Gao, W. Jie, X. Ma, X. Feng, and H. Wang, "Csi-based device-free wireless localization and activity recognition using radio image features," *IEEE Transactions on Vehicular Technology*, vol. 66, no. 11, pp. 10 346–10 356, 2017.

[12] K. Wu, X. Jiang, Y. Yi, D. Chen, and L. M. Ni, "Csi-based indoor localization," *IEEE Transactions on Parallel and Distributed Systems*, vol. 24, no. 7, pp. 1300–1309, 2013.

[13] P.-J. R. M., "Notes on the rsgb observations of the hf ambient noise floor[j]," *Radio Soc. Great Britain, Bedford, UK*, 2003.

[14] D. Zhang, Y. Liu, and L. M. Ni, "Rass: A real-time, accurate, and scalable system for tracking transceiver-free objects," *IEEE Transactions on Parallel and Distributed Systems*, vol. 24, no. 5, pp. 996–1008, 2013.

[15] J. Wang, Q. Gao, Y. Yu, P. Cheng, L. Wu, and H. Wang, "Robust device-free wireless localization based on differential rss measurements," *IEEE Transactions on Industrial Electronics*, vol. 60, no. 12, pp. 5943–5952, 2013.

[16] G. Yao, K. Huang, N. Jiang, X. Guo, Y. Li, and G. Wang, "An exponential-rayleigh model for rss-based device-free localization and tracking," *IEEE Transactions on Mobile Computing*, vol. 14, no. 3, pp. 484–494, 2015.

[17] H. Ai, K. Tang, W. Huang, S. Zhang, and T. Li, "Fast fingerprints construction via gpr of high spatial-temporal resolution with sparse rss sampling in indoor localization," *Computing*, pp. 1–14, 2019.

[18] W. Zhu, W. Zheng, and D. Zhang, "Beyond rss: A prr aided rss system to localize transceiver-free target in sparse wireless networks," in *2018 IEEE Global Communications Conference (GLOBECOM)*. IEEE, 2018, pp. 1–6.

[19] X. Wang, J. Luo, Y. Liu, S. Li, and D. Dong, "Component-based localization in sparse wireless networks," *IEEE/ACM transactions on networking*, vol. 19, no. 2, pp. 540–548, 2010.

[20] B. Sun, Y. Guo, N. Li, L. Peng, and D. Fang, "Tdl: Two-dimensional localization for mobile targets using compressive sensing in wireless sensor networks," *Computer Communications*, vol. 78, pp. 45–55, 2016.

[21] F. Garcia, J. Gomez, M. A. Gonzalez, M. Lopez-Guerrero, and V. Rangel, "Ghost: Voronoi-based tracking in sparse wireless networks using virtual nodes," *Telecommunication Systems*, vol. 61, no. 2, pp. 387–401, 2016.

[22] J. Wang, X. Zhang, Q. Gao, H. Yue, and H. Wang, "Device-free wireless localization and activity recognition: A deep learning approach," *IEEE Transactions on Vehicular Technology*, vol. 66, no. 7, pp. 6258–6267, 2017.

[23] S. Holm, "Ultrasound positioning based on time-of-flight and signal strength," in *2012 International Conference on Indoor Positioning and Indoor Navigation (IPIN)*, Nov 2012, pp. 1–6.

[24] U. L. Yong and M. Kavehrad, "Two hybrid positioning system design techniques with lighting leds and ad-hoc wireless network," *IEEE Transactions on Consumer Electronics*, vol. 58, no. 4, pp. 1176–1184, 2013.

[25] Y. Geng and K. Pahlavan, "On the accuracy of rf and image processing based hybrid localization for wireless capsule endoscopy," in *2015 IEEE Wireless Communications and Networking Conference (WCNC)*, March 2015, pp. 452–457.

[26] M. A. Bitew, R.-S. Hsiao, H.-P. Lin, and D.-B. Lin, "Hybrid indoor human localization system for addressing the issue of rss variation in fingerprinting," *International Journal of Distributed Sensor Networks*, vol. 11, no. 3, p. 831423, 2015.

[27] Y. Geng and K. Pahlavan, "Design, implementation and fundamental limits of image and rf based wireless capsule endoscopy hybrid localization," *IEEE Transactions on Mobile Computing*, vol. 15, no. 8, pp. 1951–1964, 2016.

[28] J. A. Fawcett and B. H. Maranda, "A hybrid target motion analysis/matched-field processing localization method," *Journal of the Acoustical Society of America*, vol. 94, no. 3, pp. 1363–1371, 1993.

[29] X. Huang and M. Dai, "Indoor device-free activity recognition based on radio signal," *IEEE Transactions on Vehicular Technology*, vol. 66, no. 6, pp. 5316–5329, 2017.

[30] M. Zuniga and B. Krishnamachari, "Analyzing the transitional region in low power wireless links." in *IEEE Communications Society Conference on Sensor and Ad Hoc Communications and Networks*, vol. 4, 2004, pp. 517–526.

[31] K. Vijayan, G. Ramprabu, S. S. Samy, and M. Rajeswari, "Cascading model in underwater wireless sensors using routing policy for state transitions," *Microprocessors and Microsystems*, vol. 79, p. 103298, 2020.

[32] T. Claes and D. Van Compernolle, "Snr-normalisation for robust speech recognition," in *IEEE International Conference on Acoustics, Speech, and Signal Processing Conference Proceedings*, vol. 4, 1996, pp. 331–334.

[33] N. Saleem and M. Irfan, "Noise reduction based on soft masks by incorporating snr uncertainty in frequency domain," *Circuits, Systems, and Signal Processing*, vol. 37, no. 6, pp. 2591–2612, 2018.

[34] J. Wang, H. Jiang, J. Xiong, K. Jamieson, X. Chen, D. Fang, and B. Xie, "Lifs: low human-effort, device-free localization with fine-grained subcarrier information," in *Proceedings of the 22nd Annual International Conference on Mobile Computing and Networking*. ACM, 2016, pp. 243–256.

[35] X. Corporation. Xbow corporation. [Online]. Available: http://www.xbow.com/Products/productdetails.aspx?sid=252

[36] K. Liu, X. Liu, and X. Li, "Guoguo: Enabling fine-grained indoor localization via smartphone," in *Proceeding of the 11th annual international conference on Mobile systems, applications, and services*, 2013, pp. 235–248.

[37] J. Xiong and K. Jamieson, "Arraytrack: A fine-grained indoor location system," in *Presented as part of the 10th {USENIX} Symposium on Networked Systems Design and Implementation ({NSDI} 13)*, 2013, pp. 71–84.

[38] L. M. Ni, Y. Liu, Y. C. Lau, and A. P. Patil, "Landmarc: Indoor location sensing using active rfid," in *Proceedings of the First IEEE International Conference on Pervasive Computing and Communications, 2003.(PerCom 2003)*. IEEE, 2003, pp. 407–415.

[39] Z. Yang, Z. Zhou, and Y. Liu, "From rssi to csi: Indoor localization via channel response," *ACM Computing Surveys (CSUR)*, vol. 46, no. 2, pp. 1–32, 2013.

[40] H. Wymeersch, S. Maranò, W. M. Gifford, and M. Z. Win, "A machine learning approach to ranging error mitigation for uwb localization," *IEEE transactions on communications*, vol. 60, no. 6, pp. 1719–1728, 2012.

[41] K. S. V. Prasad, E. Hossain, and V. K. Bhargava, "Machine learning methods for rss-based user positioning in distributed massive mimo," *IEEE Transactions on Wireless Communications*, vol. 17, no. 12, pp. 8402–8417, 2018.

[42] A. Conti, M. Guerra, D. Dardari, N. Decarli, and M. Z. Win, "Network experimentation for cooperative localization," *IEEE Journal on Selected Areas in Communications*, vol. 30, no. 2, pp. 467–475, 2012.

[43] M. Z. Win, Y. Shen, and W. Dai, "A theoretical foundation of network localization and navigation," *Proceedings of the IEEE*, vol. 106, no. 7, pp. 1136–1165, 2018.

[44] Z. Liu, W. Dai, and M. Z. Win, "Mercury: An infrastructure-free system for network localization and navigation," *IEEE Transactions on Mobile Computing*, vol. 17, no. 5, pp. 1119–1133, 2017.

[45] F. Meyer, T. Kropfreiter, J. L. Williams, R. Lau, F. Hlawatsch, P. Braca, and M. Z. Win, "Message passing algorithms for scalable multitarget tracking," *Proceedings of the IEEE*, vol. 106, no. 2, pp. 221–259, 2018.

[46] M. Chiani, A. Giorgetti, and E. Paolini, "Sensor radar for object tracking," *Proceedings of the IEEE*, vol. 106, no. 6, pp. 1022–1041, 2018.

[47] A. Conti, S. Mazuelas, S. Bartoletti, W. C. Lindsey, and M. Z. Win, "Soft information for localization-of-things," *Proceedings of the IEEE*, vol. 107, no. 11, pp. 2240–2264, 2019.

[48] M. Z. Win, W. Dai, Y. Shen, G. Chrisikos, and H. V. Poor, "Network operation strategies for efficient localization and navigation," *Proceedings of the IEEE*, vol. 106, no. 7, pp. 1224–1254, 2018.

[49] A. W. Tsui, Y. H. Chuang, and H. H. Chu, "Unsupervised learning for solving rss hardware variance problem in wifi localization," *Mobile Networks and Applications*, vol. 14, no. 5, pp. 677–691, 2009.

[50] Y. Liu, Y. Zhao, L. Chen, J. Pei, and J. Han, "Mining frequent trajectory patterns for activity monitoring using radio frequency tag arrays," *IEEE Transactions on Parallel and Distributed Systems (TPDS)*, vol. 23, no. 11, pp. 2138–2149, 2012.

[51] Y. Luo, K. Huang, X. Guo, and G. Wang, "A hierarchical rss model for rf-based device-free localization," *Pervasive and Mobile Computing*, vol. 31, pp. 124–136, 2016.

[52] A. Zanella, "Best practice in rss measurements and ranging," *IEEE Communications Surveys & Tutorials*, vol. 18, no. 4, pp. 2662–2686, 2016.

[53] S. Tomic, M. Beko, R. Dinis, and P. Montezuma, "Distributed algorithm for target localization in wireless sensor networks using rss and aoa measurements," *Pervasive and Mobile Computing*, vol. 37, pp. 63–77, 2017.

[54] J. Pelant, Z. Tlamsa, V. Benes, L. Polak, O. Kaller, L. Bolecek, J. Kufa, J. Sebesta, and T. Kratochvil, "Ble device indoor localization based on rss fingerprinting mapped by propagation modes," in *IEEE International Conference Radioelektronika (RADIOELEKTRONIKA)*, 2017, pp. 1–5.

[55] X. Tian, M. Wang, W. Li, B. Jiang, D. Xu, X. Wang, and J. Xu, "Improve accuracy of fingerprinting localization with temporal correlation of the rss," *IEEE Transactions on Mobile Computing*, vol. 17, no. 1, pp. 113–126, 2018.

This article has been accepted for publication in a future issue of this journal, but has not been fully edited. Content may change prior to final publication. Citation information: DOI 10.1109/TMC.2021.3063629, IEEE Transactions on Mobile Computing

JOURNAL OF LATEX CLASS FILES, VOL. 14, NO. 8, AUGUST 2015
16

[56] R. Guzmán-Quirós, A. Martínez-Sala, J. Gómez-Tornero, and J. García-Haro, "Integration of directional antennas in an rss fingerprinting-based indoor localization system," *Sensors*, vol. 16, no. 1, p. 4, 2016.

[57] X. Tian, R. Shen, D. Liu, Y. Wen, and X. Wang, "Performance analysis of rss fingerprinting based indoor localization," *IEEE Transactions on Mobile Computing*, vol. 16, no. 10, pp. 2847–2861, 2017.

[58] C.-C. Huang and H.-N. Manh, "Rss-based indoor positioning based on multi-dimensional kernel modeling and weighted average tracking," *IEEE Sensors Journal*, vol. 16, no. 9, pp. 3231–3245, 2016.

[59] C. Liu, D. Fang, Z. Yang, H. Jiang, X. Chen, W. Wang, T. Xing, and L. Cai, "Rss distribution-based passive localization and its application in sensor networks," *IEEE Transactions on Wireless Communications*, vol. 15, no. 4, pp. 2883–2895, 2016.

[60] Z. Xiong, Z. Song, A. Scalera, E. Ferrera, F. Sottile, P. Brizzi, R. Tomasi, and M. A. Spirito, "Hybrid wsn and rfid indoor positioning and tracking system," *Eurasip Journal on Embedded Systems*, vol. 2013, no. 1, pp. 1–15, 2013.

[61] H. Cho and Y. Kwon, "Rss-based indoor localization with pdr location tracking for wireless sensor networks," *AEU-International Journal of Electronics and Communications*, vol. 70, no. 3, pp. 250–256, 2016.

[62] D. M. Pozar, *Microwave engineering*. John wiley & sons, 2011.

[63] D. Zhang, J. Ma, Q. Chen, and L. M. Ni, "An rf-based system for tracking transceiver-free objects," in *Fifth Annual IEEE International Conference on Pervasive Computing and Communications (PerCom'07)*. IEEE, 2007, pp. 135–144.

[64] M. Zuniga and B. Krishnamachari, "Analyzing the transitional region in low power wireless links," in *2004 First Annual IEEE Communications Society Conference on Sensor and Ad Hoc Communications and Networks, 2004. IEEE SECON 2004.* IEEE, 2004, pp. 517–526.

[65] N. Baccour, A. Koubâa, L. Mottola, M. A. Zúñiga, H. Youssef, C. A. Boano, and M. Alves, "Radio link quality estimation in wireless sensor networks: A survey," *ACM Transactions on Sensor Networks (TOSN)*, vol. 8, no. 4, pp. 1–33, 2012.

[66] C. H. Sherman and J. L. Butler, *Transducers and arrays for underwater sound*. Springer, 2007, vol. 4.

[67] A. Bilich and K. M. Larson, "Mapping the gps multipath environment using the signal-to-noise ratio (snr). radio sci 42:rs6003," *Radio Science*, vol. 42, no. 6, pp. –, 2007.

[68] V. Niennattrakul and C. A. Ratanamahatana, "Learning dtw global constraint for time series classification," 2009.

[69] D. Zhang, K. Lu, R. Mao, Y. Feng, and L. M. Ni, "Fine-grained localization for multiple transceiver-free objects by using rf-based technologies," *IEEE Transactions on Parallel and Distributed Systems*, vol. 25, no. 6, pp. 1464–1475, 2014.

[70] J. T. Yu, M. L. Ding, and Q. Wang, "Linear location of acoustic emission source based on ls-svr and nga," *Applied Mechanics and Materials*, vol. 80-81, pp. 302–306, 2011.

[71] J.-H. Lee, D.-h. Kim, S.-N. Jeong, and S.-H. Choi, "Diagnosis and prediction of periodontally compromised teeth using a deep learning-based convolutional neural network algorithm," *Journal of periodontal & implant science*, vol. 48, no. 2, pp. 114–123, 2018.

[72] J. L. Verniero, G. G. Howes, and K. G. Klein, "Nonlinear energy transfer and current sheet development in localized alfvén wavepacket collisions in the strong turbulence limit," *Journal of Plasma Physics*, vol. 84, no. 1, pp. 905 840 103–, 2018.
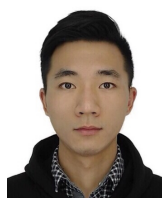
Wen Xie was born in 1996 in Jieyang City, Guangdong Province, China. He obtained a bachelor's degree in aerospace engineering from Guangzhou college of the South China University of Technology in 2018. In addition, he obtained the qualification for admission to the master's degree in engineering at Shenzhen University. His research interests include the Internet of Things and Big Data Analytics.

Zexiong Liao was born in 1996 in Shanwei City, Guangdong Province, China. He obtained a bachelor's degree in aerospace engineering from HuiZhou University in 2018. In addition, he obtained the qualification for admission to the master's degree in engineering at Shenzhen University. His research interests include the Internet of Things and Big Data Analytics.

Wenzhan Zhu received the BS degree in Computer Science and Software Engineering from Shenzhen University in 2017. His bachelor's thesis was about indoor transceiver-free localization in sparse wireless networks using PRR and RSS. He is a research assistant student. His research interests include the Internet of Things, Cloud Computing and BlockChain.

Landu Jiang received his Ph.D. in the School of Computer Science at McGill University and MSc in Computer Science from University of Nebraska-Lincoln. Besides his MSc, he is carrying out a Master degree (minor) in Construction Management. Previously, He received his BEng in Information Security Engineering from Shanghai Jiao Tong University. His research interests include computer vision, machine learning, smart sensing, wearable and mobile Computing, cyber-physical systems, green energy solutions, and online social networks.

Dian Zhang received her Ph.D. degree in computer science and engineering from the Hong Kong University of Science and Technology (HKUST), Hong Kong, in 2010. After that, she worked as a research assistant professor at the Fok Ying Tung Graduate School, HKUST. From 2012 to 2019, she worked as an associate professor at Shenzhen University. She is currently an associate professor at Lingnan University, Hong Kong. Her research interests include big data analytics and mobile computing. She is a member of the IEEE.

Yongpan Zou received his PhD degree from the department of computer science and engineering of HKUST in 2017. Since September 2017, he worked as an assistant professor in the college of computer science and software engineering of Shenzhen University. His current research interests mainly include wearable/ mobile/ubiquitous computing and HCI.